nature cell biology

DOI: 10.1038/ncb1888

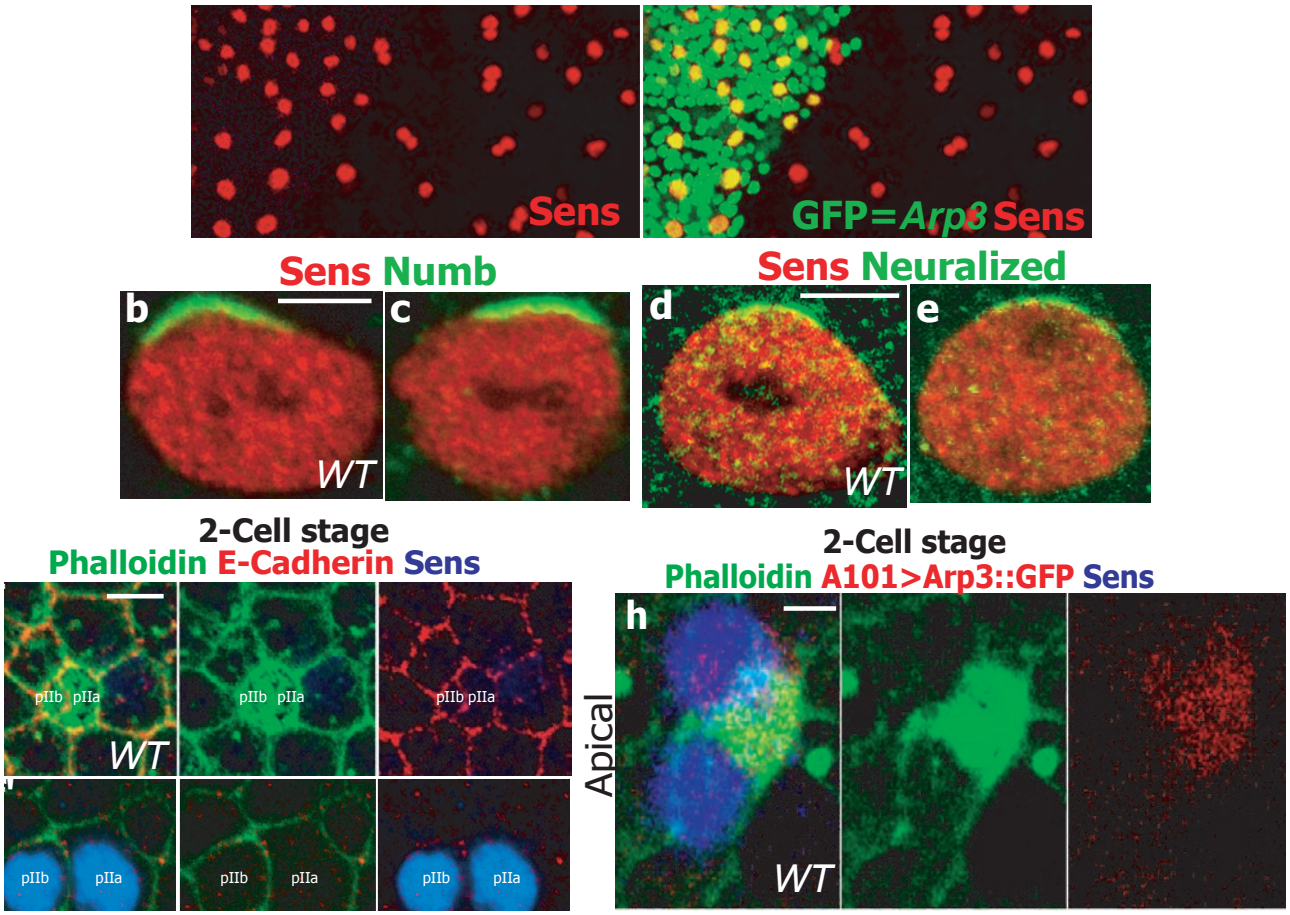

Figure S1 (**a** -**a'**) The SOPs are correctly specified in *Arp3*: (**a**) A projection of confocal sections along the XY-axis of a pupal notum at 17:30hr APF harboring *Arp3* clones marked by the presence of nuclear GFP (green) and immunostained for Sens (red) which marks the SOP and its progeny pIIa-pIIb. Note that SOPs are correctly specified in the mutant clones (green). (**b** -**e**) The segregation of asymmetric fate determinants is normal in *Arp3* mutant SOP: (**b** -**e**) Images showing a single confocal section along the XY-axis of a dividing SOP at 17:30hr APF of a *WT* or an *Arp3* pupal notum stained for asymmetric cell fate determinants (green) and Sens (red). Anterior side of the dividing SOP is oriented upwards in all these images. (**b**, **c**) Numb (green) segregates into the anterior side of the dividing SOP in both *WT* (**b**) and *Arp3* mutant clones (**c**), so that it is inherited into the anterior pIIb daughter. (**d**, **e**) Neuralized (green) segregates into the anterior side of the dividing SOP in both *WT* (d) and *Arp3* mutant clones (**e**), so that it is inherited into the anterior pIIb daughter. (**f** -**g'**) The ARS is formed only in the 2-cell stage: (**f**, **f'**) A confocal image of a single optical section along the XY-axis shows that the ARS forms above the pIIa-pIIb at the 2-cell stage. (**f**) *WT* pupal notum immunostained with phalloidin (green) reveals an apical (0.5 μm) actin enrichment, and this F-actin structure co-localizes with the apical stalk of the pIIa-pIIb cells marked by E-Cad (red). (**f'**) A basal section (~6 μm) of the sample shows the nuclei of the pIIa-pIIb cells marked with Sens (blue). (g, g') A confocal section along the XY-axis, showing immunostaining of *WT* pupal notum at the 1-cell stage with Sens (blue), phalloidin (green) and E-Cad (red). (**g**) The apical section (0.5 μm) reveals that the ARS has not yet formed at 1-cell stage. (**g'**) A basal section (6 μm) shows that the SOP, marked by Sens (blue) has not yet divided. F-actin (phalloidin–green) marks the cell membrane of the epithelial cells and SOP. (**h** -**h"**) Arp3 co-localizes with the ARS: (**h** -**h"**) Confocal images of a single optical section along the XY-axis (**h** -**h'**) and XZ-axis (**h"**) of pupal notum in which *UAS-Arp3-GFP* is expressed under the control of a *neuralized-GAL4* driver *A101-GAL4>Arp3::GFP* (red), immunostained with Sens (blue) and phalloidin (green) at the 2-cell stage. Scale bar: 10 μm in (a), 5 μm in (**f**- **g'**) and 2.5 μm in (**b**, **d**, **h**-**h"**).

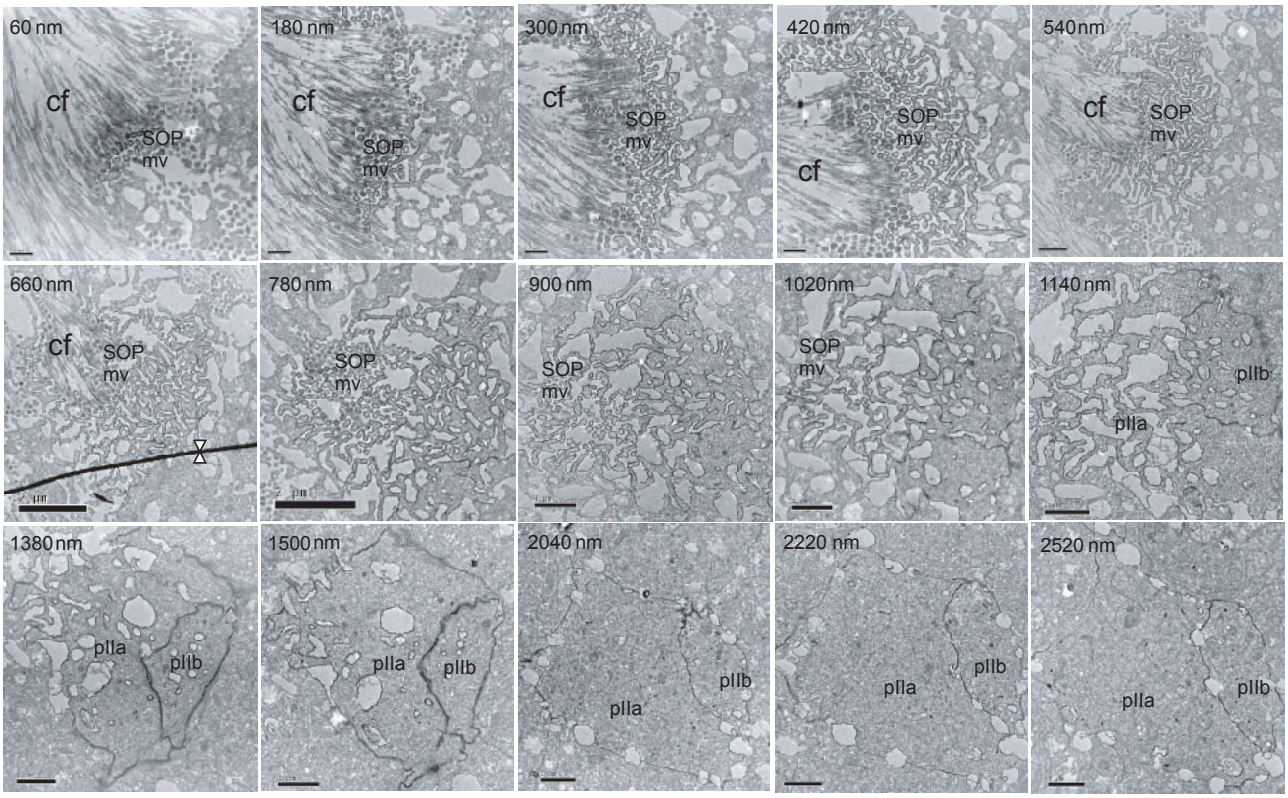

Figure S2 Transmission electron micrographs reveal the presence of finger-like projections on the apical surface of the pIIa-pIIb cells: Serial TEM micrographs of apical cross sections of pIIa-pIIb cells starting at 60 nm of the apical end through 2520 nm (basal end). Serial sections reveal the presence of numerous cross sections of finger-like projections, microvilli (mv) from 60 nm through 1020 nm. Sections from 1500 to 2520 nm show cell membrane outlines of pIIa-pIIb. The chitin fiber (cf) which assembles at the plasma membrane is a part of the apical extracellular matrix (cuticle). The dark line across 660nm with the double arrowhead is a section fold artifact.

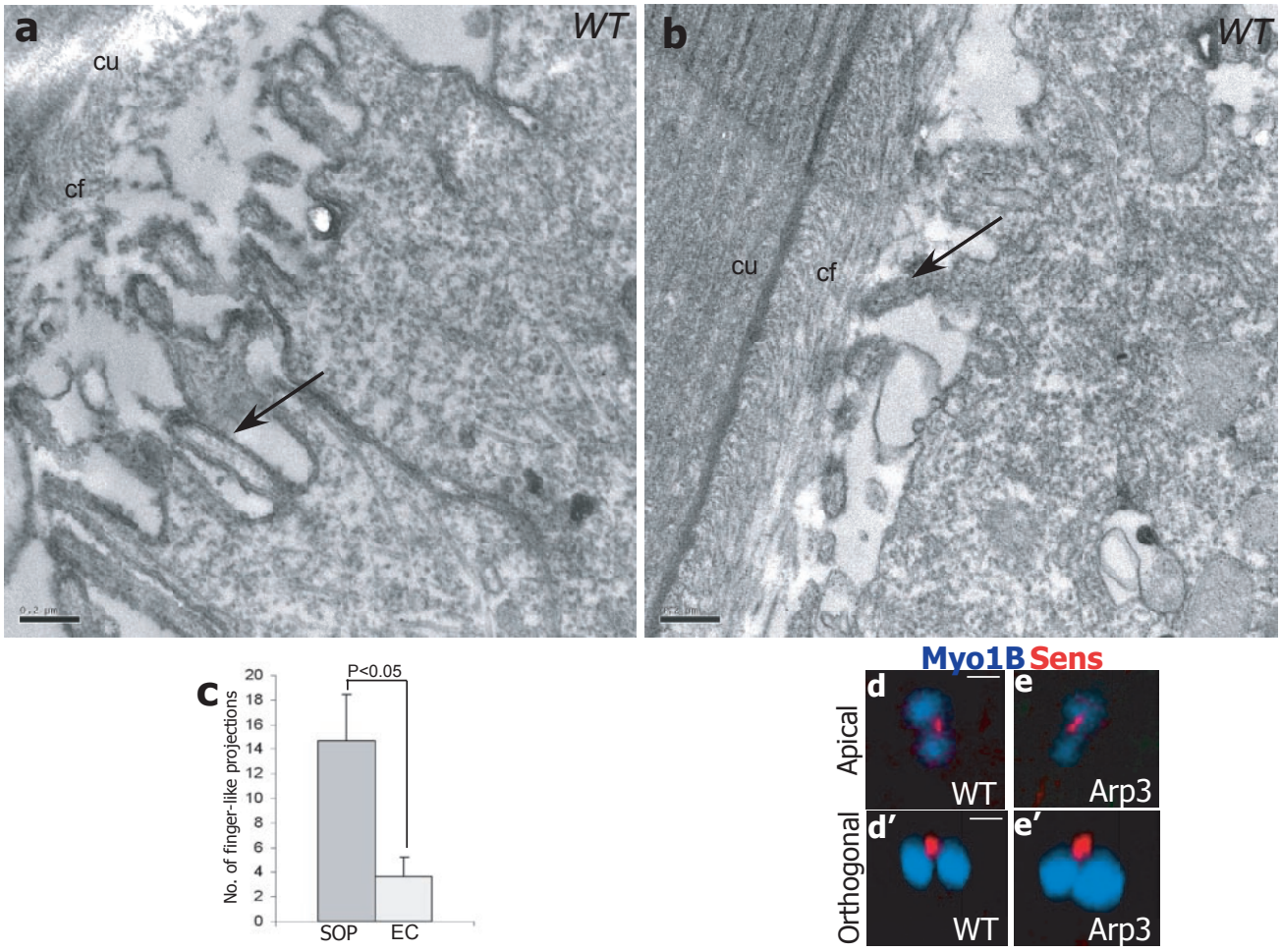

Figure S3 (**a** –**c**) The number of finger-like projections in pIIa-pIIb is significantly higher compared to those on epidermal cells: (**a**) TEM image along the XZ-axis of an SOP and (**b**) Epidermal cells at the 2-cell stage (**c**) A bar graph representing quantification of the number of finger-like projections in the epidermal cells versus the pIIa-pIIb cells. Three *WT* pIIa-pIIb pairs and six *WT* epidermal cells were used for this quantification. Arrows point to the finger-like projections. (**d** -**e'**) Microvilli marker Myo1B is correctly localized in *Arp3* mutant SOP progeny: (**d** -**e'**) Confocal images of single optical sections along the XY-axis (**d**, **e**) and the XZ-axis (**d'**, **e'**) depict immunostainings of *WT* (**d**, **d'**) and *Arp3* (**e**, **e'**) SOP progeny at the 2-cell stage, stained for Myo1B (red) and Sens (blue). Error bars indicate the SEM. Abbreviations: cuticle (cu), chitin fiber (cf). Scale bar: 0.2 µm in (**a**, **b**) and 5 µm in (**d**, **d'**).

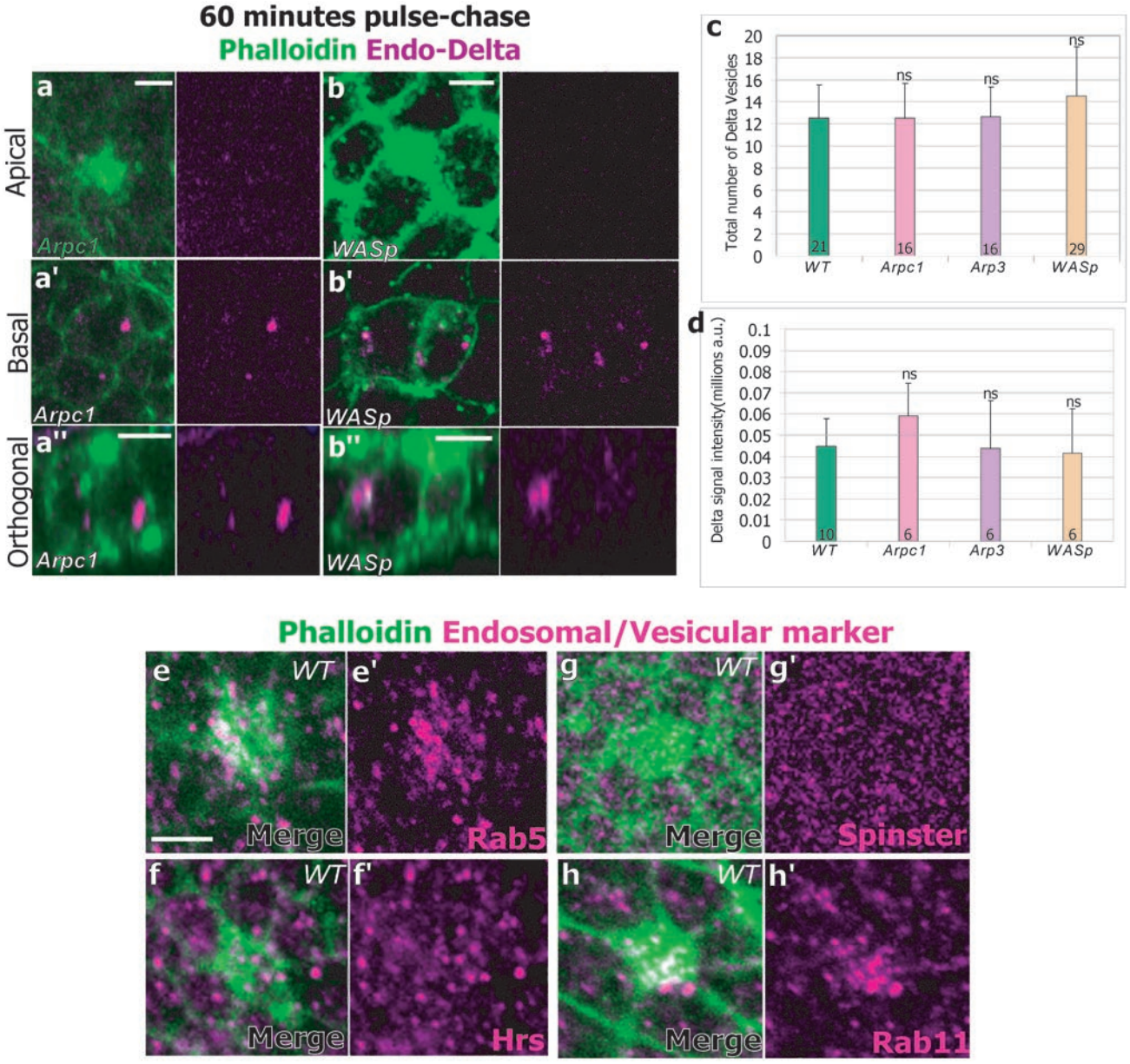

Figure S4 (**a**- **d**) Trafficking of endocytosed Delta traffics apically to the ARS after 60mins chase is compromised in *Arp2/3* and *WASp* mutants: (**a** -**b"**) Confocal images show a single section along the XY-axis (**a**, **a'**, **b**, **b'**) and XZ-axis (**a"**, **b"**) of SOP progeny at the 2-cell stage in *Arpc1* (**a**-**a"**) and *WASp* (**b**-**b"**) mutant during a 60 mins pulse-chase trafficking assay of internalized Delta–anti-Dl^{ECD} vesicles (magenta) with respect to the ARS stained by phalloidin (green). (**c**) A bar graph representing a quantification of the total number of internalized Delta vesicles which are present in the SOP progeny 60 mins after endocytosis. (**d**) A bar graph representing a quantification of the signal intensity of Delta immunostaining in the SOP progeny at 60 min chase. The number of SOP progeny (pIIa-pIIb) quantified per genotype is indicated in the bars. (**e –f'**) Early and recycling endosomes are enriched on the apical region of the ARS during fate specification: (**e** -**f'**) Confocal images of single Z-sections show immunostaining of ARS with phalloidin (green) and endosomal/vesicular markers (magenta) in *WT* pupal nota at the 2-cell stage. (**e**, **e'**) Rab5 (magenta) which marks the early endosome is enriched on the ARS (green). (**f**, **f'**) A subset of late endosomes marked by Hrs (magenta) do not show enrichment with respect to the ARS (green). (**g**, **g'**) The lysosomes marked by Spinster/ Benchwarmer (magenta) do not show enrichment relative to the ARS (green). (**e**, **e'**) Rab11 (magenta) which marks the recycling endosome is enriched with respect to the ARS (green). ns = not statistically significant. Error bars indicate SEM. Scale bar: **5** µm in (**a**, **b**, **a"**, **b"**) and 3.5 µm in (**e**).

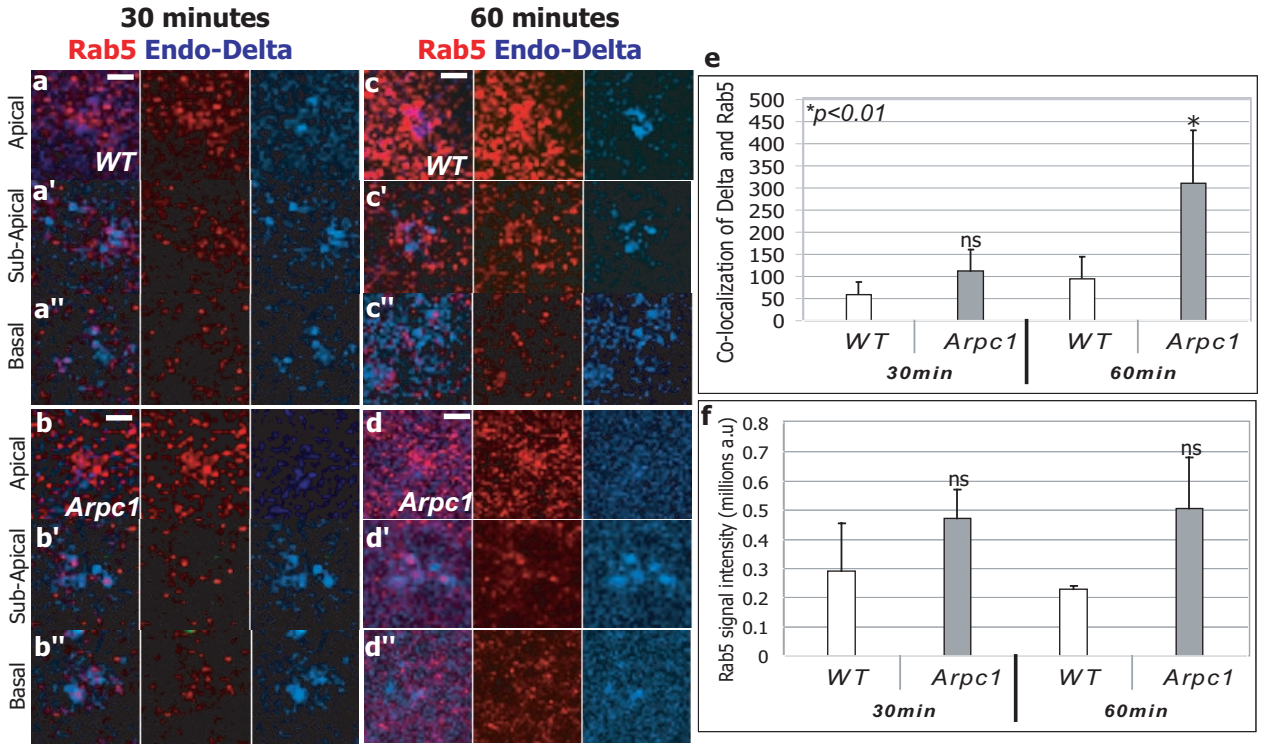

Figure S5 Pulse-chase trafficking of Delta with respect to the early endosomes (EE): Confocal images of single optical sections (**a**-**d"**) of SOP progeny at the 2-cell stage in *WT* (**a**-**a"**, **c**-**c"**) and *Arpc1* (**b**-**b"**, **d**-**d"**) after 30 mins (a-b") and 60 mins (c-**d"**) pulse-chase trafficking assays of internalized Delta–anti-DI^{ECD} (blue) with respect to the EE stained for Rab5 (red). (**a**-**d**) Apical sections (~0.5 µm) into the sample. (**a'**-**d'**) Sub-apical sections (~3 µm) into the sample. (**a"**-**d"**) Basal sections (~6 µm) into the sample. (**e**) A bar graph depicting co-localization intensity of Delta and Rab5 vesicles in arbitary units (a.u.). The measurements of signal intensities were analysed using a Student's t-test;*, p=0.01. Seven SOP progeny pairs were quantified per time point per genotype. (**f**) A bar graph depicting signal intensity of Rab5 vesicles in arbitary units (a.u.). The measurements of signal intensities were analysed using a Student's t-test;*, p=0.01. Seven SOP progeny pairs were quantified per time point per genotype. Abbreviation: ns = not statistically significant. Error bars indicate SEM. Scale bar: 3.5 µm.

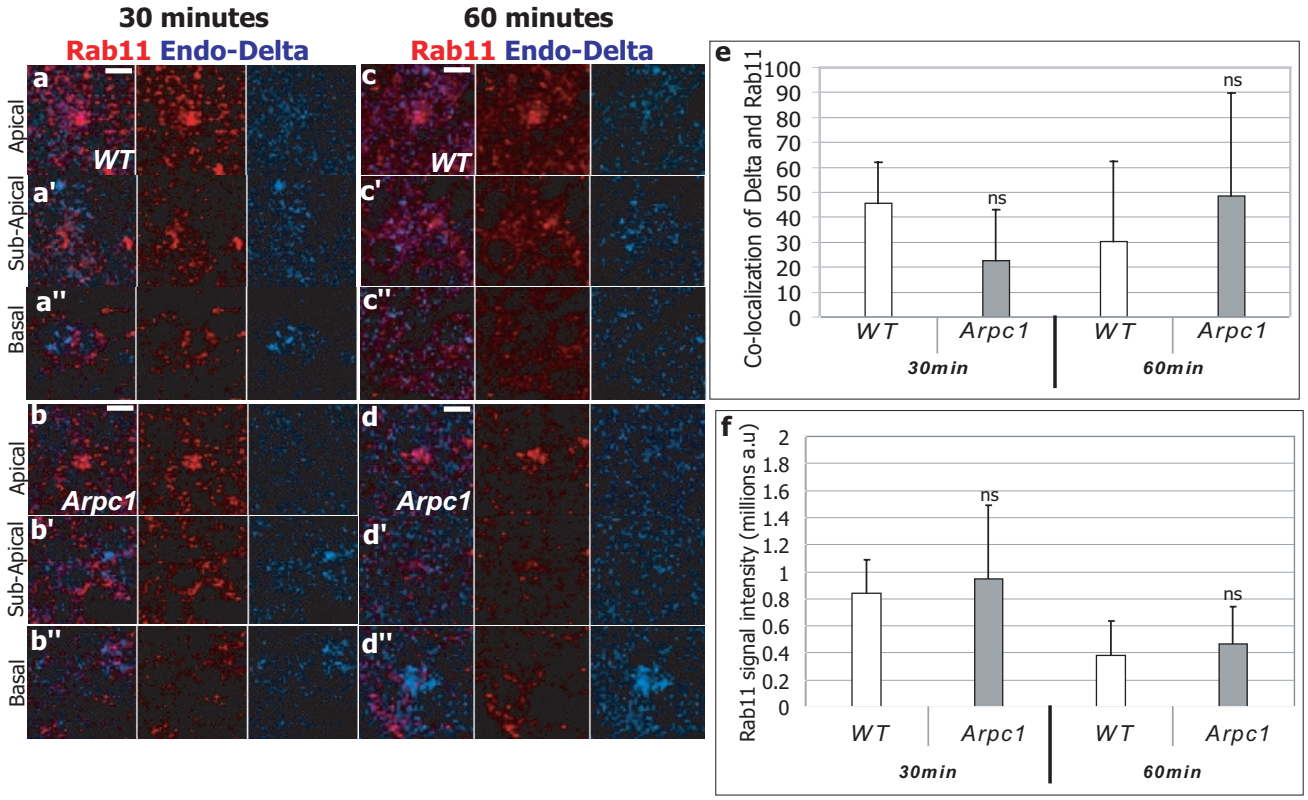

Figure S6 Pulse-chase trafficking of Delta with respect to the recycling endosomes (RE): Confocal images of single optical sections (**a**-**d”**) of SOP progeny at the 2-cell stage in *WT* (**a**-**a”**, **c**-**c”**) and *Arpc1* (**b**-**b”**, **d**-**d”**) after 30 mins (**a**-**b”**) and 60 mins (**c**-**d”**) pulse-chase trafficking assays of internalized Delta–anti-DI^{ECD} vesicles (blue) with respect to the RE stained for Rab11 (red). (**a**-**d**) Apical sections (~0.5 µm) into the sample. (**a’**-**d’**) Sub-apical sections (~3 µm) into the sample. (**a”**-**d”**) Basal sections (~6 µm) into the sample. (**e**) A bar graph depicting co-localization intensity of Delta and Rab11 vesicles in arbitrary units (a.u.). The measurements of signal intensities were analysed using a Student’s t-test;*, p=0.01. Seven SOP progeny pairs were quantified per time point per genotype. (**f**) A bar graph depicting signal intensity of Rab11 vesicles in arbitrary units (a.u.). The measurements of signal intensities were analysed using a Student’s t-test;*, p=0.01. Seven SOP progeny pairs were quantified per time point per genotype. Abbreviation: ns = not statistically significant. Error bars indicate SEM. Scale bar: 3.5 µm.

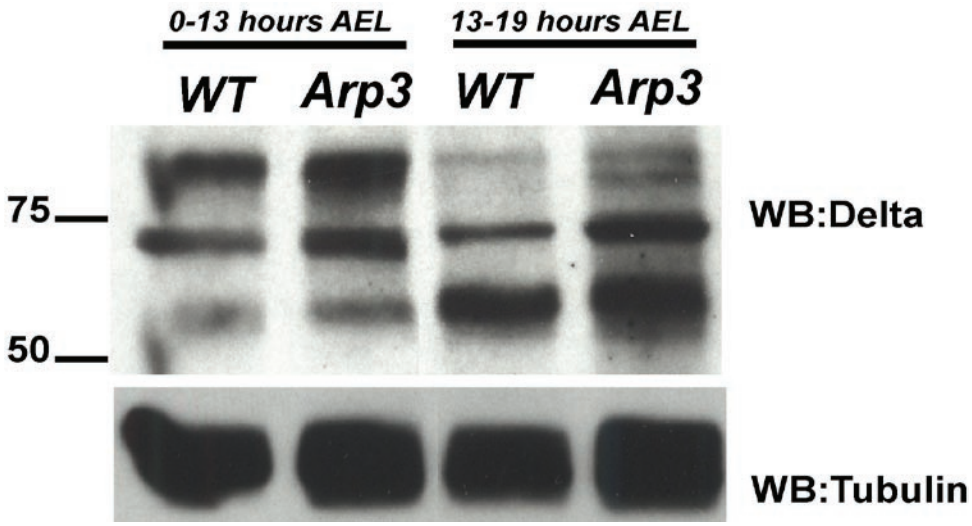

Figure S7 The processing of Delta in *Arp3* mutant embryos is unaffected: Western blotting analysis of *WT* and *Arp3* embryo lysates at 0-13hr AEL and 13-19hr AEL probed with mouse anti-Delta ascites fluid. At 0-13hr AEL note the presence of a 98 kDa band in *WT* and *Arp3* lanes. The Delta S isoform (68 kDa, is present at 0-13hr AEL but is weaker compared to the 98 kDa band. At 13-19hr AEL the 98 kDa band is much reduced in *WT* and *Arp3*. The Delta S isoform (68 kDa, arrow) is highly enriched at the 13-19 hr AEL time point in both *WT* and *Arp3* mutant. In the *Arp3* lane we sometimes observe a doublet at 98 kDa at 13-19hr AEL, but not consistently in various independent trials of the experiment.

Supplementary material:

Results:

Early and recycling endosomes are enriched on the apical region of the ARS during fate specification:

It has been proposed that Delta must be endocytosed and targeted to a specific endosomal compartment to become activated[1], possibly through a Rab11-positive recycling endosomal compartment[2, 3]. Based on our data, the ARS may have a role in these trafficking events. We therefore examined the co-localization of different endosomal compartments with respect to the ARS during cell fate specification. Immunostaining with endosomal and vesicular compartment markers including Rab5 (early endosomes, EE)[4], Rab11 (recycling endosomes, RE)[5], Hrs (late endosomes, LE)[6] and Spinster (lysosomes)[7, 8] revealed that EE and RE are enriched apically where they co-localize with the microvillar region of the ARS in the pIIa-pIIb at the 2-cell stage (Supplementary Fig. 4 e, e', h, h'). However, the LE and lysosomes are not enriched with respect to the ARS (Supplementary Fig. 4 g, g', f, f'). We find the localization of these endosomal and vesicular compartments are similar to *WT* in *Arp3, Arpc1* mutant pIIa-pIIb cells (data not shown).

Endosomal trafficking of Delta through the early endosomes (EE) and recycling endosomes (RE) during pIIa-pIIb fate specification:

To examine if Delta trafficking through the EE and RE is altered in mutants of the Arp2/3 complex, we performed pulse chase assays at 30 mins and 60 mins after

internalization (Supplementary Fig. 5, 6). We focused on these compartments as they were enriched on the ARS at the 2-cell stage (Supplementary Fig. 4 e, e', h, h'). With regard to the Rab5-positive EE compartment we find that there is no statistically significant difference of Delta co-localization with this compartment between *WT* and mutant at 30 mins post-internalization (Supplementary Fig. 5 a-b'', e). However, after 60 mins chase there seems to be a borderline significant increase in Delta vesicle co-localization to the Rab5 compartment (p=0.01, student's two-tailed test) in *Arpc1* mutants compared to *WT* (Supplementary Fig. 5 c-d'', e). We also assayed if the abundance of the EE is altered in the *Arpc1* mutant by quantifying the signal intensity of Rab5 immuno-staining in the *Arpc1* mutant pIIa-pIIb cells, 30 min and 60 mins after internalization, and we find that there is no significant difference (Supplementary Fig. 5 f).

Furthermore, we found that there is not a statistically significant difference of Delta trafficking with respect to the Rab11-positive RE at both 30 mins and 60 mins post internalization (Supplementary Fig. 6 a-d'', e). The distribution and abundance of the Rab11 compartment itself remains largely unaffected in the *Arpc1* mutants (Supplementary Fig. 6 f). In addition, when the pI cell divides, Emery et al (2005) have reported that Rab11 localizes asymmetrically to the pIIb cell[3]. We found that this asymmetric distribution of Rab11 to the pIIb compartment is unaffected in dividing pIs of *Arp3* mutants (data not shown).

Our hypothesis based on these results is that the primary defect in *Arp2/3* mutants is their inability to traffic Delta to the apical region of the ARS, and we consider this increased co-localization of Delta to the Rab5 compartment as a

secondary defect that seems to occur when the Delta vesicles do not arrive at their expected destination. The reason we favor this hypothesis is that the inability of Delta to cluster around the ARS and traffic apically seems to be a highly significant (Fig. 8g) defect as compared to a subtle increase in Delta co-localization to the Rab5 positive compartment (Supplementary Fig. 5e).

Delta processing is unaffected in *Arp3* mutants:

Wang and Struhl[1] have suggested that the internalization of Delta leads to a proteolytic cleavage in an unknown compartment. *Drosophila* full-length Delta (~98 kDa) is proteolytically processed into three different isoforms *in vivo*[9] and the short isoform Delta S (~68 kDa) may correspond to the activated form[1, 9]. During early stages of embryogenesis (0-6 hours after egg laying, hr AEL) the Delta S isoform is not generated[45]. At later developmental stages (13-24hr AEL) full-length Delta is much reduced, but the Delta S isoform is far more abundant[45]. To assay if lack of Arp2/3 function alters Delta processing we prepared lysates from *WT*, *Arp3* and *Arpc1* zygotic mutant embryos at two different developmental time periods, 0-13hr AEL and 13-19hr AEL, for western blot analysis. We find that processing of Delta is largely unaltered in *Arp3* embryos (Supplementary Fig. 7), suggesting that the processing of Delta may not depend on Arp2/3 function.